Reactivity of the Ground and Excited Spin−Orbit States for the Reaction of the $F(^2P_{3/2},^2P_{1/2})$ with D_2

Yan Zhang, Ting-Xian Xie, and Ke-Li Han*

Center for Computational Chemistry and State Key Laboratory of Molecular Reaction Dynamics, Dalian Institute of Chemical Physics, Chinese Academy of Science, Dalian 116023, China

Received: July 20, 2003; In Final Form: October 20, 2003

In this paper, we present a time-dependent quantum wave packet calculation based on the Alexander−Stark−Werner (ASW) potential energy surfaces (PESs) to study the reactivity of the ground and excited spin−orbit states for the reaction of $F(^2P_{3/2},^2P_{1/2})$ with D_2 ($v = j = 0$). The reaction probabilities and the integral cross sections are calculated. Furthermore, the multistate cross sections are compared with the single-state calculation. The multistate cross section is smaller than the single-state calculation at higher collision energy. The effect of the nonadiabatic coupling becomes more and more obvious as the collision energy increases. The overall reactivity of the excited state of F is, at most, 25% of that of the ground spin−orbit states. The threshold energy of the $F(^2P_{3/2}) + D_2$ reaction is ∼0.10 kcal/mol. The contributions of the excited state of F are 0.9% and 3.1% of the total average rate constant, at 200 and 500 K, respectively. The effect of the excited spin−orbit state rate constant to the average rate constant is very small but grows slowly as the temperature increases.

I. Introduction

The reaction of $F(^2P)$ with H_2 and its isotopic variants has had a central role in the experimental and theoretical dynamics.[1] These reactions have been extensively studied in a large variety of experiments and theoretical calculations in the past decades.[2,3] The development of high-quality ab initio potential energy surface by Stark and Werner (SW)[4] has allowed a quantitative comparison between theory and experiments. A series of quantum mechanical (QM)[5−8] and quasi-classical trajectory (QCT)[9−11] calculations on the potential energy surface (PES) are in agreement with the experimental results,[12−14] except for the detail features.

When the F atom approaches the H_2 molecule, the degeneracy of the ^2P states would be split into $^2P_{3/2}$ and $^2P_{1/2}$ states, which correlate with the reactant ground and excited spin−orbit state, respectively, as shown in Figure 1. The splitting between the two states is 1.15 kcal/mol. The spin−orbit effect increases the height of the barrier, with respect to the reactants, by 0.374 kcal/mol (one-third of the F atom spin−orbit splitting).

The role of spin−orbit and nonadiabatic effects in the F + H_2 reaction was first discussed by Tully.[15] Thereafter, various approximations were used in studying the $F(^2P) + H_2(D_2)$ system.[16−22] Schatz and co-workers applied *J*-shift approximation to calculate the state-selected and the total cumulative reaction probabilities and the thermal rate coefficients of the $Cl(^2P) + HCl$ reaction for total angular momentum $J = {}^1/_2$.[23−25] Recently, quantum-mechanical calculations on the ab inito adiabatic PES of Hartke, Stark, and Werner (HSW), including the spin−orbit corrections in the entrance channel, were conducted to investigate the $F + H_2(D_2)$ reaction.[26,27] The first exact quantum scattering calculations for the reaction of H_2 with $F(^2P_{3/2})$ and $F(^2P_{1/2})$, which accurately and completely includes the electronic angular momenta of the F atom reactant and the spin−orbit coupling, were presented by Alexander and co-workers.[28,29] Furthermore, we performed the time-dependent wave packet (TDWP)[30−33] calculations neglecting the Coriolis coupling on the Alexander−Stark−Werner (ASW) PES to investigate the nonadiabatic $F(^2P_{3/2},^2P_{1/2}) + H_2$ reaction.[34] By comparison with the exact time-independent calculations of Alexander and co-workers, it is found that the Coriolis coupling has a relatively minor role.

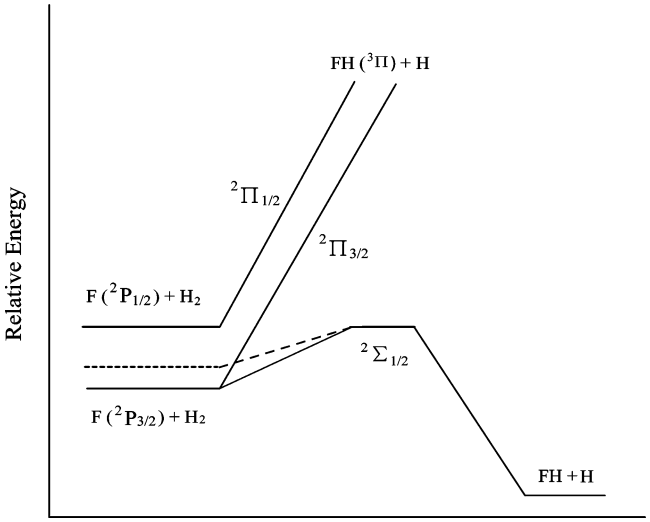

Figure 1. Energy of the $F(^2P_{3/2},^2P_{1/2}) + H_2$ reaction in collinear geometry (ref 29). Dashed line represents the single, electronically adiabatic potential surface.

However, the isotopic variant $F + D_2$ reaction has not been extensively studied using the theoretical methods. In the present work, we calculate the initial state-selected total reaction probabilities and the cross sections for the $F(^2P_{3/2},^2P_{1/2}) + D_2$ reaction on the ASW PES, using the TDWP method described in our recent work.[34] The main advantage of the TDWP approach is its slower computational scaling with the number of basis functions ($\leq N^2$ vs N^3 in the standard coupled-channel time-independent approach).[30]

* Author to whom correspondence should be addressed. E-mail: klhan@dicp.ac.cn

10.1021/jp036118u CCC: $25.00
Published on Web 11/21/2003

This paper is organized as follows. Section II briefly presents the TDWP treatment for the $F(^2P_{3/2},^2P_{1/2}) + D_2$ reaction, including the electronic angular momenta of the F atom reactant and the spin−orbit coupling. The results and discussion are presented in Section III. Section IV reports our conclusions.

II. Theory

In this section, we briefly describe the TDWP method used to calculate the initial state-selected total reaction probability of the ground and excited spin−orbit states on the ASW PES for the $F(^2P_{3/2},^2P_{1/2}) + D_2$ reaction. The method is closely related to the time-independent calculation[29] and has been used in our calculations for the $F(^2P_{3/2},^2P_{1/2}) + H_2$ reaction.[34] The total Hamiltonian in the reactant Jacobin coordinates (R,r,θ) can be written as (in atomic units, au)

$$\boldsymbol{H} = -\frac{1}{2\mu_R}\frac{\partial^2}{\partial R^2} + \frac{\boldsymbol{L}^2}{2\mu_R R^2} + \frac{\boldsymbol{j}^2}{2\mu_r r^2} + V(r,R,\theta) + V_{SO}(r,R,\theta) + h(r) \quad (1)$$

where r is the interatomic distance in the diatomic moiety, R the center-of-mass separation of the collision particles, m_R the reduced mass between atom and diatom, m_r the reduced mass of D_2, $\boldsymbol{L}$ the nuclear orbital angular momentum operator, and $\boldsymbol{j}$ the rotational angular operator of D_2. V is defined as $V_{ASW} - V_r$, where V_{ASW} is the potential of the $F(^2P_{3/2},^2P_{1/2}) + D_2$ reaction. V_{SO} is the spin−orbit interaction, and $h(r)$ is the diatomic reference Hamiltonian, which is defined as

$$h(r) = -\frac{1}{2\mu_r}\frac{\partial^2}{\partial r^2} + V_r(r) \quad (2)$$

where $V_r(r)$ is the diatomic reference potential.

The nuclear orbit angular momentum, $\boldsymbol{L}^2$, can be written as

$$\boldsymbol{L}^2 = (\boldsymbol{J} - \boldsymbol{j} - \boldsymbol{l} - \boldsymbol{s})^2 = \boldsymbol{J}^2 + \boldsymbol{j}^2 + \boldsymbol{l}^2 + \boldsymbol{s}^2 - 2\boldsymbol{J}\cdot\boldsymbol{j} - 2\boldsymbol{J}\cdot\boldsymbol{l} - 2\boldsymbol{J}\cdot\boldsymbol{s} + 2\boldsymbol{j}\cdot\boldsymbol{l} + 2\boldsymbol{j}\cdot\boldsymbol{s} + 2\boldsymbol{l}\cdot\boldsymbol{s} \quad (3)$$

where $\boldsymbol{J}$ is the total angular momentum, and $\boldsymbol{l}$ and $\boldsymbol{s}$ are the electronic orbital and spin angular momenta, respectively. The matrix elements of $\boldsymbol{L}^2$ can be determined as described in Appendix A of the recent work of Alexander and co-workers.[29]

The expansive basis functions[29,30,34] of the time-dependent wave function are

$$|n\upsilon JMKjk\lambda\sigma\rangle = \left(\frac{2J+1}{8\pi}\right)^{1/2} u_n^{\upsilon}(R)\phi_{\upsilon}(r)D_{MK}^{J*}(\Omega)y_{jk}(\hat{R},\hat{r})|\lambda\sigma\rangle \quad (4)$$

Here, $u_n^{\upsilon}(R)$ is the translational basis, $\phi_{\upsilon}(r)$ the vibrational basis, and $y_{jk}(\hat{R},\hat{r})$ the spherical harmonic. $D_{MK}^{J*}(\Omega)$ is the Winger rotation matrix element, with M being the projection of the total angular momentum along the space-frame z-axis and K being the projection of the total angular momentum along the vector $\boldsymbol{R}$ that is defined as

$$K = k + \lambda + \sigma \quad (5)$$

where k is the projection of $\boldsymbol{j}$ along the vector $\boldsymbol{R}$ and the quantities λ and σ is the projection of the electronic orbital and spin angular momenta along the vector $\boldsymbol{R}$.

To reduce the number of basis functions, the definite-parity basis functions are described as follows:

$$|n\upsilon JMKjk\lambda\sigma\epsilon\rangle = \frac{1}{\sqrt{2}}[|n\upsilon JMKjk\lambda\sigma\rangle + \epsilon|n\upsilon JM - Kj - k - \lambda - \sigma\rangle] = u_n^{\upsilon}(R)\phi_{\upsilon}(r)Y_{jKk\lambda\sigma}^{JM\epsilon} \quad (6)$$

where $\epsilon = \pm 1$ and K is positive in the definite-parity basis.

The split-operator method is used to perform the wave-packet propagation on the multiple PESs.[33] The time-dependent wave function is absorbed at the edges of the grid on every PES, to avoid artificial boundary reflection.

The initial state-selected total reaction probabilities are obtained on the PES of the ground spin−orbit state through the flux calculation[30,32]

$$P_i^J(E) = \frac{1}{\mu_r}\frac{1}{(2j+1)(2j_\alpha+1)}\mathrm{Im}\left[\left\langle \Psi_{iE}^{+}\middle|\delta(r-r_0)\frac{\partial}{\partial r}\middle|\Psi_{iE}^{+}\right\rangle\right] \quad (7)$$

where r is vibrational coordinate, i the initial state label, and E the energy label. Ψ_{iE}^{+} is the time-independent full scattering wave function. We choose the surface at $r = r_0$ for the flux evaluation.

The integral cross sections can be obtained by summing the corresponding reaction probabilities over all the partial waves (total angular momentum J):

$$\sigma_{j,j_{\alpha'},\upsilon}(E) = \frac{\pi}{k_i^2}\sum_J (2J+1)P_{,j,j_\alpha\upsilon}^{J}(E) \quad (8)$$

where $k_i = \sqrt{2\mu E}$ and E is the collision energy.

The corresponding specific rate constant k_{υ,j,j_α} can be calculated by thermally averaging the collision energy of the cross section $\sigma_{j,j_\alpha,\upsilon}(E)$ as[26]

$$k_{\upsilon,j,j_\alpha}(T) = \sqrt{\frac{8k_BT}{\pi\mu_R}}(k_BT)^{-2}\int_0^\infty E\sigma_{j,j_\alpha,\upsilon}(E)\exp\left(-\frac{E}{k_BT}\right)\mathrm{d}E \quad (9)$$

where k_B is the Boltzmann constant and E is the collision energy. Using eq 9 and the cross sections of the reaction of D_2 with $F(^2P_{3/2})$ and $F(^2P_{1/2})$, the rate constants (the initial $\upsilon = 0, j = 0$) of the ground and excited spin−orbit states, respectively, could be evaluated.

The average $\upsilon = 0$, $j = 0$ rate constant can be given by[26]

$$k_{\upsilon=0,j=0} = \frac{4}{4 + 2\exp\left(-\frac{\Delta}{k_BT}\right)}k_{\upsilon=0,j=0,j_\alpha=3/2}(T) + \frac{2\exp\left(-\frac{\Delta}{k_BT}\right)}{4 + 2\exp\left(-\frac{\Delta}{k_BT}\right)}k_{\upsilon=0,j=0,j_\alpha=1/2}(T) \quad (10)$$

The Coriolis coupling is not included in our calculation. The numerical parameters of the converged calculation are as follows: The range of the translational coordinate R is $[0.5,14.5]a_0$. The number of total translational basis is 140 (among them 60 for the interaction). The 45 vibrational basis are used to r in the range of $[0.5,6.5]a_0$. For rotational basis, $j_{max} = 30$ is used. The center of the initial wave packet is $R = 10a_0$. The width is $0.3a_0$ and the average translational energy

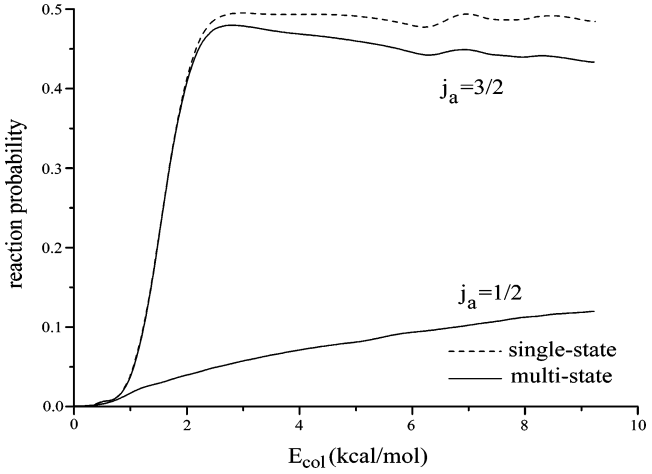

Figure 2. Multistate probabilities based on the ASW PES for the reaction of $F(^2P_{3/2,1/2})$ with D_2 ($v = j = 0$), as a function of the collision energy for $J = 0.5$ (solid line) and single-state probability for $J = 0$ (dashed line).

is 0.2 eV. The wave packets are propagated for 35 000 au for the ground spin−orbit state and for 15 000 au for the excited spin−orbit state (a time step size of 10 au is used).

III. Results

Figure 2 shows the total multistate reaction probabilities based on the ASW PES for the reaction of $F(^2P_{3/2,1/2}) + D_2$ ($v = j = 0$) as a function of the collision energy and for the total angular momenta of $J = 0.5$ and single-state probability for $J = 0$. The single-state calculations are performed on the lowest adiabatic ASW PES, which is obtained by diagonalizing the ASW potential matrix at each geometry.

As discussed by Alexander and co-workers,[29] to compare the present reaction probabilities and cross sections of the spin−orbit ground states with the single-state calculations, the single-state results must be divided by 2. As can been seen, at the low collision energy, the single-state probability is in good agreement with the multistate ground spin−orbit result. The reaction probabilities of the excited spin−orbit state are found to be small and, at most, 25% of the probabilities for the reaction of $F(^2P_{3/2})$ with D_2. The result is similar to the calculation for the reaction of $F(^2P_{3/2,1/2}) + H_2$.[29] The major difference between the probabilities for the reaction of $F(^2P_{3/2,1/2}) + H_2$ and $F(^2P_{3/2,1/2}) + D_2$ is the resonance feature. Because the PES barrier is broad enough to reduce the tunneling of the D atoms significantly, there are no resonance features in the reaction of $F(^2P_{3/2,1/2}) + D_2$.

Figure 3 shows the total multistate reaction cross sections based on the ASW PES as a function of collision energy for the $F(^2P_{3/2,1/2}) + D_2$ ($v = j = 0$) reaction and a single-state result. In the present multistate calculation, the electronic nonadiabatic potential and the spin−orbit coupling are included. Consequently, at higher collision energy, the multistate probabilities and the cross section for the $F(^2P_{3/2,1/2}) + D_2$ reaction are smaller than those of single-state calculations. As the collision energy increases, the multistate cross sections become increasingly smaller than the single-state cross sections. It seems that the effect of the nonadiabatic coupling would be obvious at high collision energy and would grow as the collision energy increases. The present results without the resonance features can be comparable to the calculation for the $F(^2P_{3/2,1/2}) + H_2$ reaction.[29,34] The integral cross sections of the ground and excited spin−orbit states for the reaction of the $F(^2P)$ with D_2 is smaller than those for the $F(^2P)$ with H_2 reaction.

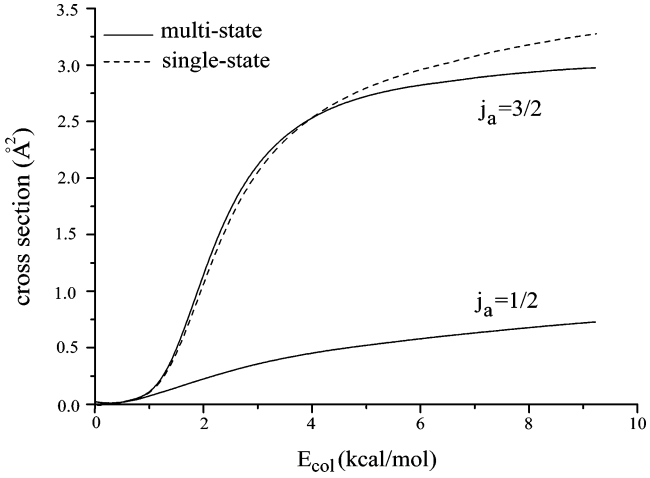

Figure 3. Total multistate cross sections for the $F(^2P_{3/2,1/2}) + D_2$ ($v = j = 0$) reaction, as a function of the collision energy (solid line) and the single-state cross section (dashed line).

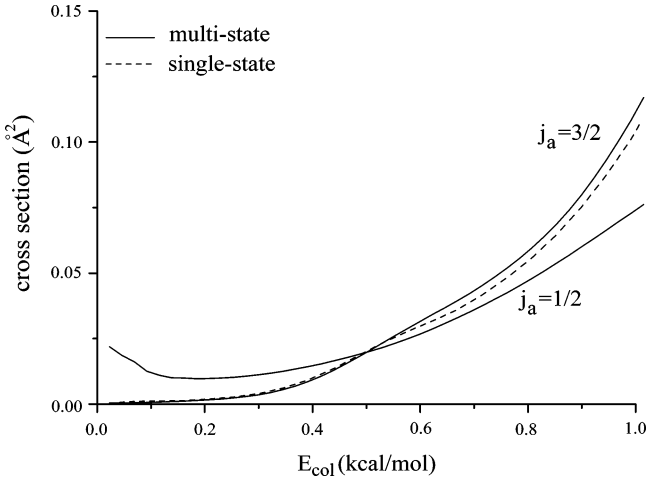

Figure 4. Total multistate cross sections for the $F(^2P_{3/2,1/2}) + D_2$ ($v = j = 0$) reaction at the very lower collision energy (solid line) and the single-state cross section (dashed line).

Figure 4 shows the cross sections for the $F(^2P_{3/2,1/2}) + D_2$ ($v = j = 0$) reaction and the single-state result at very lower collision energy. Because the excited spin−orbit state has no threshold, the reaction cross section of this state is slightly larger than that of the ground spin−orbit state at this low collision energy. As the collision energy becomes higher, the cross sections of the ground spin−orbit states rapidly increase. In the collision energy range of Figure 5, the agreement between the multistate cross section and the single-state calculation is almost perfect.

A threshold of the ground spin−orbit state and single-state reaction appears at ∼0.10 kcal/mol. The threshold can be compared with the QM value of ∼0.36 kcal/mol (15 meV) obtained on the HSW PES[24] and the QCT value of ∼0.92 kcal/mol (40 meV) obtained on the SW PES.[11] The present threshold of the ground spin−orbit states is lower than the result obtained on the HSW PES.

Figure 5 shows the comparison between the average $v = 0$, $j = 0$ rate constant obtained through eq 10 and the rate constant obtained through eq 9 for the reaction of $F(^2P_{3/2,1/2}) + D_2$. In the calculation using eq 9, it is assumed that 100% of the F atoms were in either the ground or excited spin−orbit states. The ground spin−orbit rate constant obtained through eq 9 agrees well with the average value. Thus, the contribution of the excited spin−orbit rate constant to the average value seems

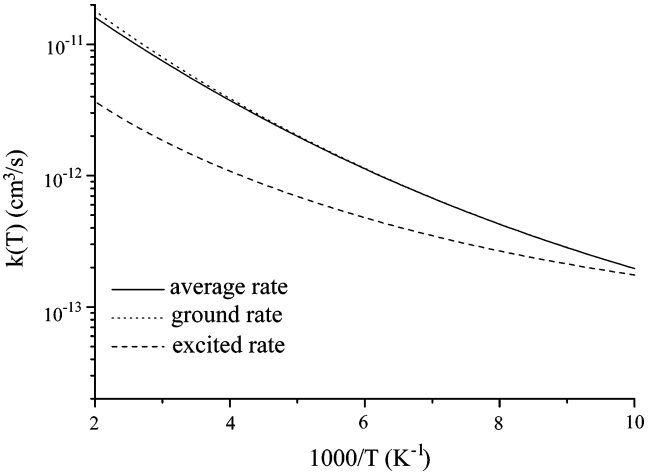

Figure 5. Average $v = 0$, $j = 0$ rate constant obtained through (—) eq 10, (···) eq 9 for the reaction of $F(^2P_{3/2}) + D_2$, and (---) eq 9 for the reaction of $F(^2P_{1/2}) + D_2$.

to be very small. At 200 K, if only the ground spin−orbit state reaction would occur, the rate constant would be 2.029×10^{-12} cm^3/s. Comparing with the total average rate constant, $k_{v=0,j=0}(T) = 1.994 \times 10^{-12}$ cm^3/s, we can see that the contribution of the excited spin−orbit state is very little, as small as only 0.9% of the total average rate constant. The effect of the excited spin−orbit states grows slowly as the temperature increases. At 500 K, the contribution of the excited spin−orbit states could reach 3.1% of the total average rate constant.

IV. Conclusion

The time-dependent wave packet (TDWP) calculation based on the Alexander−Stark−Werner (ASW) potential energy surface (PES) has been performed to study the reactivity of the ground and excited spin−orbit states for the reaction of $F(^2P_{3/2},^2P_{1/2})$ with D_2 ($v = j = 0$). The Coriolis terms are not included. The integral cross sections are determined by summing the corresponding reaction probabilities over all the partial waves.

The reaction probabilities of the ground and excited spin−orbit state for $J = 0.5$ are presented. The reactivity of the excited spin−orbit states is small and, at most, 25% of that of the ground spin−orbit states. The comparison between the cross sections of the multistate and the single-state results indicates that, at higher collision energy, the cross sections of the ground spin−orbit state on the ASW PES for the reaction of F with D_2 are smaller than the single-state calculation. The effect of the nonadiabatic coupling would grow as the collision energy increases. The present threshold of the ground spin−orbit state is ~0.10 kcal/mol and is smaller than that on the HSW PES. The contribution of the excited spin−orbit state rate constant to the average value is very small and grows slowly as the temperature increases. The contributions of the excited spin−orbit state rate constant are 0.9% and 3.1% of the total average value, at 200 and 500 K, respectively.

Acknowledgment. This work is supported by NSFC (Grant No. 20028304) and NKBRSF (Grant No. 1999075302). We would like to thank Xin Zhang for his assistance on computers.

References and Notes

(1) Levine, R. D., Bernstein, R. B., Eds. *Molecular Reaction Dynamics and Chemical Reactivity*; Oxford University Press: New York, 1987.
(2) Manolopoulos, D. E. *J. Chem. Soc., Faraday Trans.* **1997**, *93*, 673.
(3) Castillo, J. F.; Manolopoulos, D. E. *Faraday Discuss* **1998**, *110*, 119.
(4) Stark, K.; Werner, H.-J. *J. Chem. Phys.* **1996**, *104*, 6515.
(5) Castillo, J. F.; Manolopoulos, D. E.; Stark, K.; Werner, H.-J. *J. Chem. Phys.* **1996**, *104*, 6531.
(6) Zhang, D. H.; Lee, S. Y.; Baer, M. *J. Chem. Phys.* **2000**, *112*, 9802.
(7) Skodje, R. T.; Skouteris, D.; Manolopoulos, D. E.; Lee, S.-H.; Dong, F.; Liu, K. *Phys. Rev. Lett.* **2000**, *85*, 1206.
(8) Honvault, P.; Launay, J. M. *Chem. Phys. Lett.* **1998**, *287*, 270.
(9) Aoiz, F. J.; Bañares, L.; Herrero, V. J.; Rábanos, V. S.; Stark, K.; Werner, H.-J. *J. Chem. Phys.* **1995**, *102*, 9248.
(10) Martínez-Haya, B.; Aoiz, F. J.; Bañares, L.; Honvault, P.; Launay, J. M. *Phys. Chem. Chem. Phys.* **1999**, *1*, 3415.
(11) Faubel, M.; Martínez-Haya, B.; Rusin, L. Y.; Tappe, U.; Toennies, J. P. *J. Chem. Phys. A* **1997**, *101*, 6415.
(12) Faubel, M.; Martínez-Haya, B.; Rusin, L. Y.; Tappe, U.; Toennies, J. P.; Aoiz, F. J.; Bañares, L. *J. Chem. Phys. A* **1998**, *102*, 8695.
(13) Dong, F.; Lee, S.-H.; Liu, K. *J. Chem. Phys.* **2000**, *113*, 3633.
(14) Skodje, R. T.; Skouteris, D.; Manolopoulos, D. E.; Lee, S.-L.; Dong, F.; Liu, K. *J. Chem. Phys.* **2000**, *112*, 4536.
(15) Tully, J. C. *J. Chem. Phys.* **1974**, *60*, 3042.
(16) Rebentrost, F.; Lester, W. A., Jr. *J. Chem. Phys.* **1977**, *67*, 3367.
(17) Meyer, H.-D.; Miller, W. H. *J. Chem. Phys.* **1979**, *71*, 2156.
(18) Fitz D. E.; Kouri, D. J. *J. Chem. Phys.* **1981**, *74*, 3933.
(19) Lepetit, B.; Launay, J. M.; Dourneuf, M. L. *Chem. Phys.* **1986**, *106*, 111.
(20) Gilibert, M.; Baer, M. *J. Phys. Chem.* **1994**, *98*, 12822.
(21) Gilibert, M.; Baer, M. *J. Phys. Chem.* **1995**, *99*, 15748.
(22) Billing, G. D.; Rusin, L. Y.; Sevryuk, M. B. *J. Chem. Phys.* **1995**, *103*, 2482.
(23) Schatz, G. C. *J. Phys. Chem.* **1995**, *99*, 7522.
(24) Maierle, C. S.; Schatz, G. C.; Gordon, M. S.; McCabe, P.; Connor, J. N. L. *J. Chem. Soc., Faraday Trans.* **1997**, *93*, 709.
(25) Schatz, G. C.; McCabe, P.; Connor, J. N. L. *Faraday Discuss. Chem. Soc.* **1998**, *110*, 139.
(26) Aoiz, F. J.; Bañares, L.; Castillo, J. F. *J. Chem. Phys.* **1999**, *111*, 4013.
(27) Honvault, P.; Launay, J. M. *Chem. Phys. Lett.* **1999**, *303*, 657.
(28) Alexander, M. H.; Werner, H.-J.; Manolopoulos, D. E. *J. Chem. Phys.* **1998**, *109*, 5710.
(29) Alexander, M. H.; Manolopoulos, D. E.; Werner, H.-J. *J. Chem. Phys.* **2000**, *113*, 11084.
(30) Zhang, D. H.; Zhang, J. Z. H. *J. Chem. Phys.* **1994**, *101*, 1146.
(31) Zhang, J. Z. H. *J. Chem. Phys.* **1991**, *94*, 6047.
(32) Zhang, D. H.; Zhang, J. Z. H. *J. Chem. Phys.* **1994**, *101*, 3671.
(33) Xie, T.-X.; Zhang, Y.; Zhao, M.-Y.; Han, K.-L. *Phys. Chem. Chem. Phys.* **2003**, *5*, 2034.
(34) Zhang, Y.; Xie, T.-X.; Han, K.-L.; Zhang, J. Z. H. *J. Chem. Phys.*, in press.